Available online at www.sciencedirect.com
ScienceDirect
Engineering Fracture Mechanics 75 (2008) 1736–1752
Engineering Fracture Mechanics
www.elsevier.com/locate/engfracmech

A finite fracture mechanics approach to structures with sharp V-notches ☆

A. Carpinteri [a], P. Cornetti [a,*], N. Pugno [a], A. Sapora [a,b], D. Taylor [b]

[a] *Dipartimento di Ingegneria Strutturale e Geotecnica, Politecnico di Torino, Turin, Italy*
[b] *Department of Mechanical and Manufactural Engineering, Trinity College, Dublin, Ireland*

Received 28 November 2006; received in revised form 21 March 2007; accepted 3 April 2007
Available online 19 April 2007

Abstract

Criteria assuming that failure of quasi-brittle materials is affected by the stresses acting over a finite distance from the crack tip are widely used inside the scientific community. For instance, they have been applied to predict the failure load of specimens containing sharp V-notches, assuming as a critical parameter the average stress ahead the notch tip. However, this kind of approaches disregards energy balance considerations, which, as well known, are the basis of linear elastic fracture mechanics (LEFM). In order to overcome these drawbacks, the present paper uses a recently introduced finite fracture mechanics (FFM) criterion, i.e. a fracture criterion assuming that crack grows by finite steps. The length of this finite extension is determined by a condition of consistency of both energy and stress requirements; as a consequence, the crack advancement is not a material constant but a structural parameter. The criterion is applied to structures with sharp V-notches. The expression of the generalized fracture toughness, which is a function of material tensile strength, fracture toughness and notch opening angle, is given analytically. Finally, we provide comparisons with: (i) the experimental data we obtained from testing Polystyrene specimens under three point bending; (ii) some experimental data available in the literature. The agreement between theoretical predictions and experimental results is generally satisfactory and, for most of the cases analyzed, the FFM predictions are better than the ones provided by the simple average stress approach.

Keywords: Finite fracture mechanics; V-notches; Fracture toughness; Tensile strength

1. Introduction

When dealing with brittle or quasi-brittle materials, two main failure criteria are generally taken into account. The former is a stress criterion: i.e. failure takes place if, at least in one point, the maximum principal

☆ This article appeared in its original form in *Fracture of Nano and Engineering Structures: Proceedings of the 16th European Conference of Fracture, Alexandroupolis, Greece, July 3–7, 2006* (Edited by E.E. Gdoutos, 2006). Springer, Dordrecht, The Netherlands. ISBN 1-4020-4971-4.

* Corresponding author. Tel.: +39 0115644901; fax: +39 0115644899.
E-mail addresses: alberto.carpinteri@polito.it (A. Carpinteri), pietro.cornetti@polito.it (P. Cornetti), nicola.pugno@polito.it (N. Pugno), alberto.sapora@polito.it (A. Sapora), dtaylor@tcd.ie (D. Taylor).

0013-7944/$ - see front matter
doi:10.1016/j.engfracmech.2007.04.010

stress reaches the tensile strength σ_u. The latter is an energetic criterion: it states that failure happens if the crack driving force $\mathscr{G}$ equals the crack resistance $\mathscr{G}_F$. $\mathscr{G}_F$ is the so-called fracture energy, i.e. the energy necessary to create the unit fracture surface. According to Irwin's relationship and dealing, for the sake of simplicity, only with mode I crack propagation, the energetic criterion can be expressed equivalently in terms of stress intensity factor (SIF) K_I and fracture toughness K_{Ic}: failure is achieved whenever $K_I = K_{Ic}$. This is the failure criterion provided by linear elastic fracture mechanics (LEFM).

The stress criterion provides good results only for crack-free bodies, whereas the energetic criterion works only for bodies containing a sufficiently large crack. Otherwise both the criteria fail. In fact, the stress criterion provides a null failure load for a body containing a crack, the stress field being singular in front of the crack tip; symmetrically, the energetic criterion provides an infinite failure load for a crack-free body, the stress intensity factor being zero in absence of a crack. The above mentioned criteria therefore work for the extreme cases (i.e. no crack or large crack); problems are expected when they are applied to intermediate cases, such as, for instance, short cracks, blunt cracks or sharp notches.

Let us consider more in detail the case of specimens with a sharp V-notch (sometimes referred to as re-entrant corner), which is the subject of the present paper. In this case both the stress and energetic criteria fail since the stress field is singular at the notch tip but with a order of the singularity lower than 1/2, which implies a null SIF. As a consequence, the stress criterion provides a vanishing failure load; at the same time, the energy criterion yields a critical load tending to infinity. This example shows clearly that the stress and the energy approach have to be somehow coupled in order to gather a general validity.

Concerning numerical applications to quasi-brittle materials, the goal of coupling the two above mentioned approaches has been achieved by means of the fictitious crack model introduced by Hillerborg et al. [12], which takes into account both the tensile strength and the fracture energy of the given material. The fictitious crack model, as well as the cohesive crack model [4], requires a specific numerical algorithm to be inserted in structural design codes, thus providing a very versatile tool for the analysis of quasi-brittle material structures. For what concerns the application of the cohesive crack model to V-notched specimens, a detailed analysis can be found in the recent paper by Gómez and Elices [9].

Anyway, easier criteria can be put forward by introducing a material length, which allows one to get analytical results, at least with sufficiently simple geometries, or to couple the failure criterion with a linear elastic analysis performed numerically, for instance by the finite element method. The task of the characteristic length is to take into account the fracture toughness for stress based criteria and the tensile strength for energy based criteria. We will show how in the following section.

2. Finite fracture mechanics

Let us consider a specimen where the crack of length a (already present or not, i.e. $a \geqslant 0$) will grow in the x direction under mode I condition as soon as critical conditions are met. The origin of the orthogonal coordinate system (x, y) is placed at the point where crack will propagate as in the specimen of Fig. 1.

A stress based failure criterion can be set assuming that failure takes place when the average stress ahead of the crack tip over a Δ_S-long segment reaches the critical value σ_u. Or, equivalently, when the force resultant over a segment of length Δ_S in front of the crack tip reaches the critical value $\sigma_u \Delta_S$. In formulae:

$$\int_0^{\Delta_S} \sigma_y(x)\,\mathrm{d}x = \sigma_u \Delta_S \tag{1}$$

Obviously, this criterion provides $\sigma = \sigma_u$ for a crack-free specimen under a tensile load (and without stress gradient). On the other hand, the value of the material length must be determined imposing the LEFM

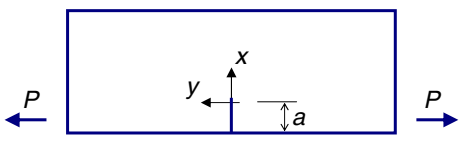

Fig. 1. Specimen subjected to mode I loading condition. The origin of the cartesian frame is placed at crack tip, x being the direction of crack growth.

criterion $K_I = K_{Ic}$ for a specimen containing a relatively large crack ($a \gg \Delta_S$). In such a case, only the asymptotic stress field at the crack tip $\sigma_y(x) = K_I/\sqrt{2\pi x}$ is required; its substitution in Eq. (1) provides the length of the segment the stress must be averaged on:

$$\Delta_S = \frac{2}{\pi}\left(\frac{K_{Ic}}{\sigma_u}\right)^2 \tag{2}$$

If an analytical solution is not available, the stress field to be inserted in (1) can be obtained numerically, e.g. by a standard finite element analysis.

The stress criterion is sometimes referred to as "average stress criterion" or "line method" and the length Δ_S as "critical distance"; it dates back to Neuber and Novozhilov [21,22]. Afterwards, several researchers applied this criterion in a wide range of geometries and materials: see, for instance, notch analysis [24,30,6], fatigue problems [28] and composite materials [32].

Symmetrically, the LEFM criterion can be modified in order to provide the same result as the stress criterion for the limit case of plain specimens. We simply assume that failure is achieved when the energy available during a Δ_E-long crack extension reaches the critical value $\mathcal{G}_F\Delta_E$. This can be expressed as

$$\int_a^{a+\Delta_E} \mathcal{G}(a)\,da = \mathcal{G}_F\Delta_E \tag{3}$$

or, according to Irwin's relationship:

$$\int_a^{a+\Delta_E} K_I^2(a)\,da = K_{Ic}^2\Delta_E \tag{4}$$

Obviously, this criterion coincides with the LEFM criterion $K_I = K_{Ic}$ for a specimen containing a relatively large crack ($a \gg \Delta_E$). On the other hand, the value of the material length must be determined imposing $\sigma = \sigma_u$ for a vanishing crack ($a = 0$). In such a case, considering only through cracks for two-dimensional geometries, the asymptotic value for the stress intensity factor is given by $K_I = c\sigma\sqrt{\pi a}$, where c is a dimensionless factor equal to 1 for center cracks and equal to 1.122 for edge cracks (which is, for instance, the case of the specimen in Fig. 1) and σ is the opening stress acting at the point where crack will grow. Substituting this expression in Eq. (4) allows the determination of Δ_E:

$$\Delta_E = \frac{2}{\pi}\left(\frac{K_{Ic}}{c\sigma_u}\right)^2 \tag{5}$$

Note that the crack extensions (2)–(5) for the stress and energy criteria are the same for a center crack but slightly differ for an edge crack. Furthermore, the simulations performed till now have shown that the predictions of the two criteria [29] are usually close but not identical.

From a computational point of view, it is worth pointing out that, if the critical load is required for several crack lengths a, the energy criterion (4) is much easier to apply than the stress criterion (1) as long as the SIF vs. a functions are available in the SIF handbooks (or numerically by specific LEFM codes). In fact the stress function $\sigma_y(x)$ to be inserted into Eq. (1) (usually not available analytically) has to be computed for *each* value of a, whereas only one function, $K_I(a)$, is needed to determine the critical load by means of Eq. (4) for *every* value of a.

Although there are some differences, the physical meaning of the two criteria (1)–(4) is the same: fracture does not propagate continuously but by a finite crack extension, whose length is a material constant. Hence, the framework is a finite fracture mechanics (FFM) approach.

The energy FFM criterion (4) contains as a particular case (vanishing crack increments) the classical LEFM. It should be noted, however, that for a material with finite strength and toughness, FFM cannot predict a stable, continuous crack growth, whereas the cohesive crack model can. On the other hand, from a physical point of view, it should be noted that several (perhaps all) fracture processes involve discontinuous crack growth rather than smooth, continuous growth, at least at the beginning of the cracking phenomenon (see, e.g., [1] for metals, [16] for polymers and [11] for bones). These crack jumps are likely related to material microstructure (i.e. barrier spacing or grain boundaries), giving rise to material instabilities such as snap

backs. However, these microstructural processes are far from being completely understood and, in what follows, the finite extension of a crack will be assumed *a priori*.

The energy criterion as expressed by Eq. (4) was developed in [23], under the heading quantized fracture mechanics (where its validity for nano-structures and microscopic specimens was established) and in [29], where it was named finite fracture mechanics. These two papers have demonstrated that the approach can be used for all classes of materials, at all size scales from point defects in carbon nanotubes to large notches in engineering structures. Note that the term FFM has been already used by [10,15] in a different framework, i.e. the multiple cracking of coating layers and of composite laminates. In those cases, the term finite refers to the creation of new cracks of (although small) finite size. In spite of the different context, it was decided to use the same name since the idea to substitute the infinitesimal increase of crack surface with a finite increment is the same both for our and their approach. Finally, note that a slightly different form of the energy criterion (4) has been introduced by Seweryn [25] within the analysis of V-notched components.

In spite of the fact that criteria (1) and (4) provide predictions generally in good agreement with experimental data, it has been shown by Cornetti et al. [7] that they still contain some flaws. They arise if we consider specimens whose structural size is close to the finite crack extensions (2)–(5).

Let us consider for instance a three point bending (TPB) un-notched specimen with a ligament length equal to the finite crack extension. The resultant of the stresses acting over the ligament is null; hence the average stress criterion (1) provides an infinite failure load. On the other hand, the energy available at constant load is infinite: the integral at the right-hand side of Eq. (4) diverges and therefore the critical load predicted is zero. Both the predictions are obviously unacceptable: it is argued that sound predictions can be obtained only for specimen heights one order of magnitude larger than the finite crack extension. Unfortunately, this is not always the case, especially for materials with a large critical distance, as, e.g., concrete-like materials.

In order to overcome these drawbacks, a new FFM criterion has been proposed by Cornetti et al. [7], where it was applied to the prediction of size effect upon strength of TPB cracked and un-cracked specimens. Comparison with experimental data on concrete beams [13] proved the soundness of the approach, which is briefly recalled hereafter and applied to V-notched specimens in the following section.

According to the criteria (1)–(4), the internal lengths Δ_S and Δ_E are determined imposing the fulfilment of limit cases: long crack failure load for the stress-based criterion and no crack failure load for the energy-based criterion. Nevertheless, the two approaches remain distinct and the fulfilment of one of them usually implies the violation of the other one. In other words, when applying the average stress criterion, the energy released in the crack extension is not always $\mathcal{G}_F\Delta_S$: hence the energy balance is violated (under the assumption that the kinetic energy associated with the dynamics of crack growth is negligible). On the other hand, when applying the energetic criterion, the resultant of the stresses acting on the crack extension can differ from the product $\sigma_u\Delta_E$. In order to overcome this incongruence, the hypothesis that Δ is a material constant has to be removed. Note that the crack is still propagating by finite steps, i.e. we remain in the framework of FFM. The value of the finite crack extension is determined by the contemporaneous fulfilment of stress and energy criteria, i.e. when both the following equations are satisfied:

$$\begin{cases} \int_0^{\Delta_{SE}} \sigma_y(x)\,\mathrm{d}x = \sigma_u\Delta_{SE} \\ \int_a^{a+\Delta_{SE}} K_I^2(a)\,\mathrm{d}a = K_{Ic}^2\Delta_{SE} \end{cases} \tag{6}$$

This means that failure takes place whenever there is a segment of length Δ_{SE} over which the stress resultant is equal to $\sigma_u\Delta_{SE}$, and, contemporarily, the energy available for that crack extension is equal to $\mathcal{G}_F\Delta_{SE}$. Eq. (6) represents a system of two equations in the two unknowns: σ_f, i.e. the failure load (implicitly embedded in the functions $\sigma_y(x)$ and $K_I(a)$), and Δ_{SE}, i.e. the crack extension. While each single equation represents only a necessary condition for failure, the fulfilment of both of them represents a necessary and sufficient condition for fracture to propagate. From a physical point of view, the criterion expressed in Eq. (6) is equivalent to state that fracture is energy driven but a sufficiently high stress field must act in order to trigger crack propagation. Since the present fracture criterion is obtained by coupling the stress and energy FFM criteria (Eqs. (1)–(4)), henceforth, we will refer to Eqs. (6) as the *coupled FFM criterion*. As will be shown in Section 3, the length Δ_{SE} ceases to be a material constant and becomes a structural parameter, thus able to take into account the interaction between the finite crack extension and the geometry of the specimen.

Finally, among recent advances in the analysis of V-notched structures, we want to cite: the failure criterion proposed by Lazzarin and Zambardi [17], which assumes as a critical parameter the strain energy in a small region around the notch tip; the fracture criterion proposed by Leguillon [18,19], which is similar to Eq. (6) (it differs because it is based on the point-wise stress criterion); the promising technique proposed by Tovo et al. [31], where the critical parameter is a non-local equivalent stress expressed by an implicit differential equation; the paper by Kashtanov and Petrov [14], where an intriguing idea to extend Griffith's energy balance to V-notched structures is set by means of a *fractal* crack growth.

3. Generalized fracture toughness for a V-notch

In this section, the coupled FFM criterion (6) is applied to the strength prediction of TPB specimens with a V-notch at mid-span. We are interested in the variation of the strength along with the notch opening angle ω.

As well-known from Williams' analysis, geometries with re-entrant corners show a stress field singularity weaker than 1/2, this value being typical of cracked configurations. Therefore, as already stated in the Introduction, both the strength ($\sigma = \sigma_u$) and the toughness ($K_I = K_{Ic}$) criteria do not succeed in predicting failure of V-notched components. We will show that FFM can overcome the drawbacks of classical failure criteria.

The coefficient of the leading term in the asymptotic expansion of the stress field in the neighborhood of the corner tip is named *generalized* stress intensity factor and marked by K_I^* henceforth [3]. In formulae this means that, if we consider a symmetrical (with respect to x-axis) geometry such as the one of Fig. 2, the asymptotic stress field ahead the notch tip on the axis of symmetry is provided by:

$$\sigma_y(x) = \frac{K_I^*}{(2\pi x)^{1-\lambda}} \tag{7}$$

where λ is an exponent which depends on the angle ω according to the classical work by Williams: $\lambda = \lambda(\omega)$. Observe that, varying ω, the physical dimensions of K_I^* change. For the sake of clarity, it should be highlighted that also other definitions of the generalized SIF are used in the literature: their difference lies in the exponent of the term (2π) at the right-hand side of Eq. (7). Some authors prefer to raise that term to 0 (as in [18]) or to 1/2 (as in [17] or [26]) instead of $(1-\lambda)$. However, the use of the definition corresponding to the expression (7) has the nice property that the generalized SIF coincides respectively with the SIF and the stress at the notch tip in the extreme cases of a crack and a flat edge.

If the crack advancement Δ is small enough with respect to the other geometrical quantities, the stress field to be inserted into Eq. (1) or (6) is sufficiently well described by its leading term (Eq. (7)). Let us consider firstly the average stress criterion. Substituting Eq. (7) into Eq. (1) shows that critical conditions are achieved when the generalized SIF reaches the critical value K_{Ic}^*:

$$K_I^* = K_{Ic}^* \tag{8}$$

where [24]

$$K_{Ic}^* = \lambda \frac{(2K_{Ic})^{2(1-\lambda)}}{\sigma_u^{1-2\lambda}} \tag{9}$$

and it is named generalized fracture toughness [3].

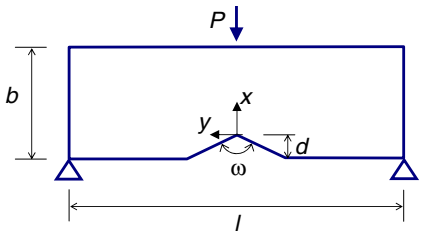

Fig. 2. Three point bending (TPB) test of a V-notched specimen.

Observe that not only the value but also the physical dimensions ($[F][L]^{-(1+\lambda)}$, $F=$ force, $L=$ length) of the generalized fracture toughness vary along with the notch opening angle: the extreme cases are the flat edge ($\omega=\pi$, $\lambda=1$), when K^*_{Ic} coincides with the tensile strength σ_u, and the crack ($\omega=0$, $\lambda=\frac{1}{2}$), when K^*_{Ic} becomes the fracture toughness K_{Ic}.

When failure is governed by Eq. (8), i.e. when the generalized SIF is the critical parameter [3,8], the structural behavior is defined to be brittle. We showed that this statement is a consequence of the smallness of the finite crack advancement with respect to the specimen size. This means that brittleness is more a structural property rather than a material property. Brittle collapse will proceed ductile collapse not only if the material has low toughness and a high strength (i.e. the material is brittle), but also if the structural size is large. In other words, a typical brittle material can show a ductile behavior if the structural size is small enough or, vice-versa, a typical ductile material can show a brittle behavior if the structural size is large enough. In formulae, this concept is very well summarized by introducing the brittleness number s:

$$s=\frac{K_{Ic}}{\sigma_u\sqrt{b}} \tag{10}$$

where b is a size characteristic of the structure. The brittleness number s is a non-dimensional quantity introduced by Carpinteri [2]: brittle structural behaviors are generally expected for low brittleness numbers.

Concerning V-notched specimens, theoretical predictions provided by the average stress criterion are usually satisfactory [24]. Nevertheless, from a physical point of view, Eq. (8) coupled with Eq. (9) is not very convincing since an energy background is missing. On the other hand, as well known, the LEFM criterion $K_I=K_{Ic}$, valid for cracked bodies, derives from an energy balance, the SIF being related to the strain energy release rate $\mathcal{G}$ by Irwin's relationship $K_I=\sqrt{\mathcal{G}E}$. According to the average stress criterion, Eq. (8) lacks this energy counterpart.

Our aim is now to apply the coupled FFM criterion (6) to symmetrical specimens with sharp V-notches, i.e. loaded in mode I. It will be shown that FFM provides an energetic meaning to Eq. (8) and, at the same time, yields a different estimate of the generalized fracture toughness with respect to Eq. (9).

In order to use Eq. (6), the SIF for a short crack of length a growing from the notch tip is required (see Fig. 3a). This function is not available in the literature, but it can be obtained from the weight functions providing the SIF for a crack at a V-notch tip of an infinite plate loaded by a pair of forces acting on the crack lips (see Fig. 4). It should be observed that this geometry is not the actual one. Nevertheless the solution for the specimen geometry tends to coincide with the one for the infinite plate for sufficiently small cracks. This is exactly what happens in the present case since, assuming a brittle structural behavior (low brittleness number), the finite crack extension is much shorter than the other specimen geometrical quantities.

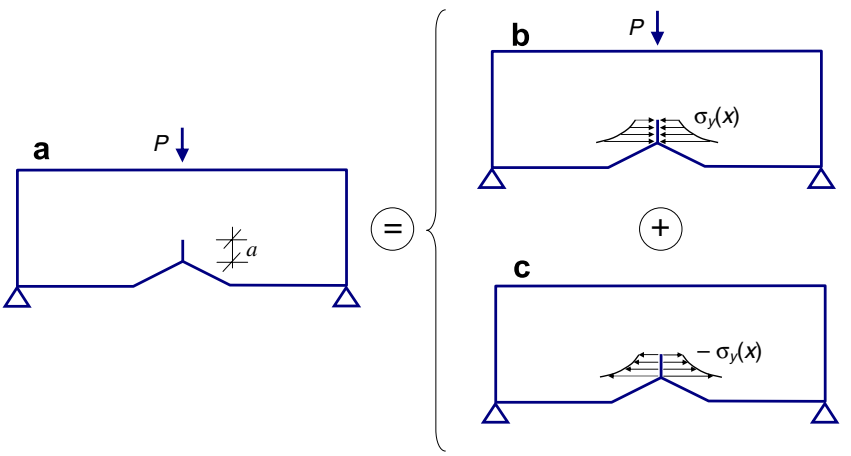

Fig. 3. Principle of effect superposition to determine the SIF of a crack at a notch tip. The SIFs of the schemes (a) and (c) are equal and the stress distribution of schemes (b) and (c) are given by Eq. (7). Observe that the geometry (b) coincides with the un-cracked case of Fig. 2.

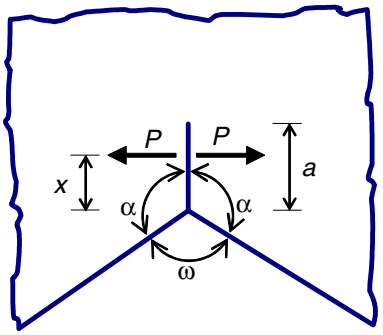

Fig. 4. Crack at a V-notch tip loaded by a pair of forces P.

The SIF for a pair of forces P is [27]:

$$K_{\mathrm{I}} = P\sqrt{\frac{2}{\pi a}}F\left(\frac{x}{a},\alpha\right) \tag{11}$$

with

$$F\left(\frac{x}{a},\alpha\right) = \frac{\tilde{f}(\alpha) + \frac{x}{a}\tilde{g}(\alpha) + \left(\frac{x}{a}\right)^2\tilde{h}(\alpha)}{\sqrt{1-\frac{x}{a}}} \tag{12}$$

where $\alpha = \pi - \omega/2$ (see Fig. 4). The expressions of the functions $\tilde{f},\tilde{g},\tilde{h}$ are as follows:

$$\tilde{f}(\alpha) = \sqrt{\frac{\pi}{2}}\sqrt{\frac{2\alpha+\sin 2\alpha}{\alpha^2-\sin^2\alpha}} \tag{13a}$$

$$\tilde{g}(\alpha) = -1 - 3\tilde{f}(\alpha) + \tilde{f}_1(\alpha) \tag{13b}$$

$$\tilde{h}(\alpha) = 2 + 2\tilde{f}(\alpha) - \tilde{f}_1(\alpha) \tag{13c}$$

with:

$$\tilde{f}_1(\alpha) = \frac{6.142 + 2.040\alpha^2 - 0.1290\alpha^3}{\alpha^{\frac{3}{2}}} \tag{14}$$

Eq. (11) can be seen as a weight function, since it allows one to determine the SIF for any stress field $\sigma_y(x)$ acting on the crack faces:

$$K_{\mathrm{I}}(a) = \int_0^a \sigma_y(x)\sqrt{\frac{2}{\pi a}}F\left(\frac{x}{a},\alpha\right)\mathrm{d}x \tag{15}$$

The principle of effect superposition can now be invoked to determine the SIF of the geometry in Fig. 3a. In fact the geometry we are dealing with can be seen as the sum of the two cases of Figs. 3b and c, where the crack faces are subjected to the stress field of the un-cracked specimen, i.e. Eq. (7). In the former scheme (Fig. 3b) the stresses cause crack closure, whereas in the latter one (Fig. 3c) they tend to open the crack lips. It is evident that the first case correspond to the un-cracked (but notched) configuration, i.e. the geometry in Fig. 2, where the SIF is null. Hence the SIF of the second scheme (Fig. 3c) coincides with the SIF of the geometry we are interested in (Fig. 3a). Note that, since we use only the asymptotic stress field (7), this argument is valid as far as the crack length a is short with respect to all geometrical quantities, i.e. specimen height b, length l and notch depth d; however, these requirements are fulfilled since we assumed a brittle structural behavior.

The SIF of the geometry of Fig. 3c can be obtained substituting the stress field (7) into Eq. (15), yielding:

$$K_{\mathrm{I}}(a) = \psi(\omega)\frac{K_{\mathrm{I}}^*}{(2\pi)^{1-\lambda}}a^{\lambda-\frac{1}{2}} \tag{16}$$

where

$$\psi(\omega) = \int_0^1 \sqrt{\frac{2}{\pi}} \frac{F(t,\alpha)}{t^{1-\lambda}}\,\mathrm{d}t \tag{17}$$

$t = x/a$ being a dummy variable. Function ψ depends only on the notch opening angle ω through α and λ. Solving the integral in Eq. (17) provides the following analytical expression for ψ:

$$\psi(\omega) = \sqrt{\frac{2}{\pi}}\left[\tilde{f}(\alpha)B\left(\lambda,\frac{1}{2}\right) + \tilde{g}(\alpha)B\left(\lambda+1,\frac{1}{2}\right) + \tilde{h}(\alpha)B\left(\lambda+2,\frac{1}{2}\right)\right] \tag{18}$$

where B is the beta function. Function ψ is plotted vs. ω in Fig. 5.

According to what was stated above, Eq. (16) provides the expression of the SIF not only for the geometry of Fig. 3c, but also for the geometry of Fig. 3a, i.e. the SIF for a crack at a V-notch tip loaded in mode I. Observe that the SIF K_I is a function of the generalized SIF K_I^* for the un-cracked configuration, of the notch opening angle ω and of the crack length a. Concerning the dependence on the crack length, it is worthwhile to observe that Eq. (16) encompasses the limit case of an edge crack, $K_I \propto \sqrt{a}$ ($\omega = \pi$, $\lambda = 1$) and a pre-existing crack, $K_\mathrm{I} \propto a^0$, i.e. constant ($\omega = 0$, $\lambda = \frac{1}{2}$). This last result is coherent with the assumption $a \ll d$: in fact, since the crack a is much shorter than the notch depth d, if the notch becomes a crack we have $K_\mathrm{I}(d+a) \cong K_\mathrm{I}(d)$.

Note that a formula analogous to Eq. (16) providing the energy required for creating a small crack at a V-notch tip has been recently derived by Leguillon [18]. He exploited a different technique (i.e. the theory of asymptotic matching); however, he did not provide an analytic expression for the SIF of a crack at a notch tip as we did here by means of Eqs. (16) and (18). Furthermore, according to the authors' knowledge, the exponent of the power law between the crack driving force and the length of a crack at a V-notch tip dates back to the work by Morozov [20].

We are now able to apply the coupled FFM criterion (6). We need to substitute Eqs. (7) and (16) into the system (6). Analytical passages provide the values of the finite crack extension Δ_SE:

$$\Delta_\mathrm{SE} = \frac{2}{\lambda\psi^2}\left(\frac{K_\mathrm{Ic}}{\sigma_u}\right)^2 \tag{19}$$

and the critical value of the generalized SIF (i.e. the generalized toughness):

$$K_\mathrm{Ic}^* = \lambda^\lambda\left[\frac{4\pi}{\psi^2}\right]^{(1-\lambda)}\frac{K_\mathrm{Ic}^{2(1-\lambda)}}{\sigma_u^{1-2\lambda}} = \xi(\omega)\frac{K_\mathrm{Ic}^{2(1-\lambda)}}{\sigma_u^{1-2\lambda}} \tag{20}$$

where function $\xi(\omega)$ is introduced for the sake of simplicity. Observe that both the finite crack extension Δ_SE and the generalized toughness K_Ic^* are functions of the material parameters and of the notch opening angle (ψ and λ are functions of ω). Therefore, as it should have been expected from the general framework outlined in Section 2, the finite crack extension Δ_SE is a *structural* property since it depends on the material (through K_Ic

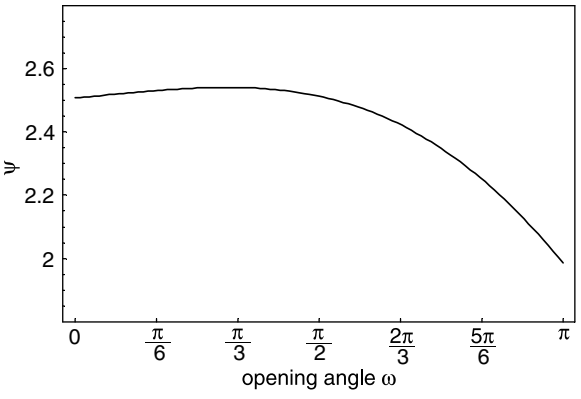

Fig. 5. Function ψ vs. notch opening angle ω. It varies from $\sqrt{2\pi} \cong 2.51$ for $\omega = 0$ to $1.12\sqrt{\pi} \cong 1.99$ for $\omega = \pi$.

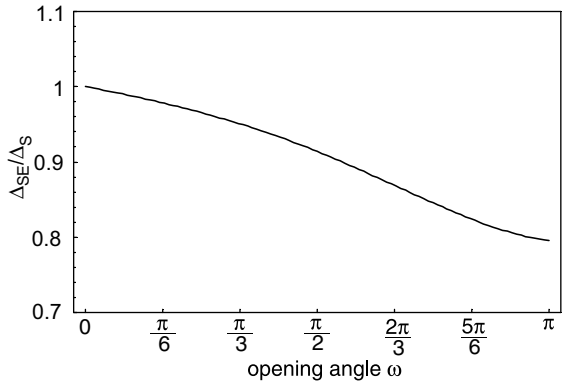

Fig. 6. Ratio between the finite crack extension Δ_{SE} and the characteristic length Δ_S of the average stress criterion. Observe that the finite crack extension Δ_{SE} varies from Δ_S for $\omega = 0$ to Δ_E for $\omega = \pi$, i.e. the ratio varies from 1 to $1.12^{-2} \cong 0.797$.

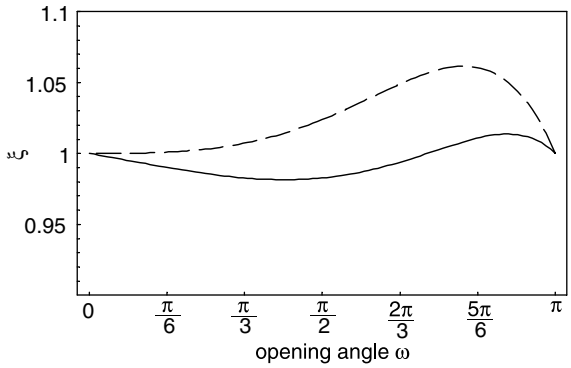

Fig. 7. Function ξ vs. notch opening angle ω according to the FFM coupled criterion (continuous line) and to the average stress criterion (dashed line).

and σ_u) as well on the geometry (through ω). More in detail, as highlighted in Fig. 6, the finite crack extension varies from Δ_S for $\omega = 0$ to Δ_E for $\omega = \pi$.

Function ξ is plotted vs. ω in Fig. 7, where, for the sake of comparison, also the value of ξ corresponding to the generalized fracture toughness (9) estimated by the average stress criterion is drawn (i.e. $\xi = \lambda 4^{1-\lambda}$). Since ξ is equal to 1 for ω equal to 0° and 180°, Eq. (20) shows that the generalized fracture toughness is intermediate between the strength and the toughness. This feature is obviously shared with the expression of K^*_{Ic} provided by the average stress criterion (i.e. Eq. (9)). However, by means of Eq. (20), the criterion (8) gained a deeper physical consistency with respect to the average stress criterion, since it now derives from energy balance considerations.

Finally, observe that the extension of the present fracture criterion to mixed mode problems is not straightforward, since, in such cases, it is necessary to determine firstly the crack orientation. On the other hand, in spite of a weaker (according to the authors' opinion) physical background, failure criteria such as [17,31] are easily extended to mixed mode problems since they do not pay attention to the direction of crack growth.

4. Computation of the generalized stress intensity factor

Once the specimen geometry is set, in order to apply the FFM criterion proposed in the previous Section, it is necessary to know the generalized SIF K^*_I for a unit load. Then, by means of Eqs. (8)–(20), the load causing failure is readily established.

The value of K_I^* can be achieved by different methods, usually starting from a finite element analysis (FEA) of the geometry to be analyzed. The simplest method (but not the most accurate) is to observe that, by definition, K_I^* is the coefficient of the leading term of the stress expansion in the neighborhood of the corner, see Eq. (7). Hence K_I^* can be determined by comparing Eq. (7) with the stress field obtained by a FEA. The method can be further improved [8] by considering the displacement field (function of K_I^* as well) instead of the stress field, since the FEA provides better approximations for the displacement values than for the stress ones.

However, some problems arise when dealing with this kind of approach: standard FEAs are not able to catch the stress singularity at the notch tip, thus providing incorrect values in its neighborhood. Furthermore, it is not clear over which interval the stress field must be considered if one aims to determine K_I^*, since, after a certain distance from the tip, other terms than the asymptotic one contribute to the stress values.

In order to avoid such problems, more accurate methods can be set on the basis of *path independent integrals*, which allow to work far from the notch tip. More in detail we will make use of the so called *H*-integral, whose computational procedure is outlined in [26] and briefly sketched in the following.

For the sake of simplicity, only mode I configurations will be dealt with. Let us fix (Fig. 8a) a cartesian (x,y) and a polar (r,θ) reference system whose origin is at the notch tip. As well known from Williams' analysis the generic stress σ and displacement η components show the following power law dependencies on r in the neighborhoods of the tip:

$$\sigma = \mathrm{O}(r^{-1+\lambda}), \quad r \to 0 \tag{21a}$$

$$\eta = \mathrm{O}(r^{\lambda}), \quad r \to 0 \tag{21b}$$

where λ is the eigenvalue characterizing the only singular stress field possible at the re-entrant corner. That is, λ is the root of the following transcendental equation $(0 < \lambda < 1)$:

$$\sin 2\lambda\alpha = -\lambda \sin 2\alpha \tag{22}$$

We may observe that, if λ is a solution of Eq. (22), so is $-\lambda$. It means that there exists a *complementary* stress-displacement $(\tilde{\sigma},\tilde{\eta})$ field that satisfies the two-dimensional stress equations of equilibrium in absence of body forces as well as the stress-free conditions on the notch faces and whose dependence on r is given by

$$\tilde{\sigma} \propto r^{-1-\lambda} \tag{23a}$$

$$\tilde{\eta} \propto r^{-\lambda} \tag{23b}$$

Let us indicate by $\{t_n\}$ the stress vector acting on a segment with unit normal vector $\{n\}$ and by $\{\eta\}$ the displacement vector. By $[\sigma]$ we mark the two-dimensional stress tensor, so that $\{t_n\} = [\sigma]\{n\}$. Referring to the actual and complementary stress-displacement fields, we can now apply Betti's reciprocal theorem to state that, in absence of body forces, the identities of mutual works yields:

$$\int_{\mathscr{C}} \{\eta\}^{\mathrm{T}} \{\tilde{t}_n\}\, \mathrm{d}s = \int_{\mathscr{C}} \{\tilde{\eta}\}^{\mathrm{T}} \{t_n\}\, \mathrm{d}s \tag{24}$$

where $\mathscr{C}$ is any closed contour inside the plane region occupied by the elastic plate, s the curvilinear abscissa defined upon the contour in a counter-clockwise sense and $\{n\}$ is directed outward. From Eq. (24), it follows:

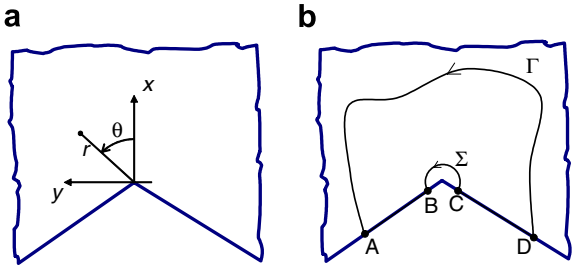

Fig. 8. Computation of the generalized SIF at a V-notch tip: (a) cartesian and polar reference system; (b) integration paths.

$$\int_{\mathscr{C}} (\{\eta\}^{\mathrm{T}}[\tilde{\sigma}] - \{\tilde{\eta}\}^{\mathrm{T}}[\sigma])\{n\}\,\mathrm{d}s = 0 \tag{25}$$

We can now choose as integration path the closed contour composed by the line Γ, the segments on notch flanks AB and CD and the arc of circumference Σ (see Fig. 8b), whose center is at notch tip. Because of the boundary conditions, the integrand vanishes along notch faces. Therefore, we have (the senses of integration are displayed in Fig. 8b):

$$\int_{\Gamma} (\{\eta\}^{\mathrm{T}}[\tilde{\sigma}] - \{\tilde{\eta}\}^{\mathrm{T}}[\sigma])\{n\}\,\mathrm{d}s = \int_{\Sigma} (\{\eta\}^{\mathrm{T}}[\tilde{\sigma}] - \{\tilde{\eta}\}^{\mathrm{T}}[\sigma])\{n\}\,\mathrm{d}s \tag{26}$$

This relationship holds for every line Γ starting from a flank and ending onto the other one. In other words the integral at the left hand side is *path-independent*; it is named H_{I}-integral (the subscript I is because of mode I loading conditions).

Next, we shrink the arc of the circumference Σ toward the notch tip, where the actual stress-displacement field has the behavior provided by Eqs. (21). Note that, along the circumference Σ, $\mathrm{d}s = r\mathrm{d}\theta$. Furthermore, because of Eqs. (21)–(23), the integral at the right hand side of Eq. (26) is made by terms of the kind $\eta\tilde{\sigma}r \approx \tilde{\eta}\sigma r \approx r^0 = \text{constant}$. This means that the integral along Σ (i.e. the H-integral) is proportional to the generalized SIF. The complementary stress field is defined up to a multiplicative constant (the generalized complementary SIF $\widetilde{K}^*_{\mathrm{I}}$). Hence $\widetilde{K}^*_{\mathrm{I}}$ can be chosen in such a way that $H_{\mathrm{I}} = K^*_{\mathrm{I}}$, thus providing the following formula for the computation of the generalized stress intensity factor K^*_{I}:

$$H_I = K^*_{\mathrm{I}} = \int_{\Gamma} (\{\eta\}^{\mathrm{T}}[\tilde{\sigma}] - \{\tilde{\eta}\}^{\mathrm{T}}[\sigma])\{n\}\,\mathrm{d}s \tag{27}$$

where the complementary stress-displacement fields are given, in polar coordinates, by the following formulae (valid under plane strain conditions):

$$\tilde{\sigma}_r = -\widetilde{K}^*_I r^{-1-\lambda}[(\lambda+3)\cos(\lambda+1)\theta - \beta\cos(\lambda-1)\theta] \tag{28a}$$

$$\tilde{\sigma}_\theta = \widetilde{K}^*_I r^{-1-\lambda}[(\lambda-1)\cos(\lambda+1)\theta - \beta\cos(\lambda-1)\theta] \tag{28b}$$

$$\tilde{\tau}_{r\theta} = -\widetilde{K}^*_I r^{-1-\lambda}[(\lambda+1)\sin(\lambda+1)\theta - \beta\sin(\lambda-1)\theta] \tag{28c}$$

$$\tilde{u}_r = \frac{\widetilde{K}^*_I r^{-\lambda}}{2G\lambda}[(\lambda+3-4\nu)\cos(\lambda+1)\theta - \beta\cos(\lambda-1)\theta] \tag{28d}$$

$$\tilde{u}_\theta = \frac{\widetilde{K}^*_I r^{-\lambda}}{2G\lambda}[(\lambda-3+4\nu)\sin(\lambda+1)\theta - \beta\sin(\lambda-1)\theta] \tag{28e}$$

The first three quantities are the normal and tangential components of the symmetric stress tensor $[\tilde{\sigma}]$ and the last two are the components of the displacement vector $\{\tilde{\eta}\}$. G is the shear modulus and ν the Poisson's ratio. Furthermore:

$$\widetilde{K}^*_{\mathrm{I}} = \frac{\pi G\lambda}{1-\nu}\frac{\lambda\sin^2\alpha + \sin^2\lambda\alpha}{\sin 2\alpha + 2\alpha\cos 2\lambda\alpha} \tag{29a}$$

$$\beta = \frac{\lambda^2 - 1}{\lambda\cos 2\alpha + \cos 2\lambda\alpha} \tag{29b}$$

Eqs. (28) and (29) can be found in [26]. They were slightly modified because of the different definition of generalized SIF we adopted (i.e. $\sigma_y = K^*_{\mathrm{I}}/(2\pi x)^{1-\lambda}$ as in Eq. (7) instead of $\sigma_y = K^*_{\mathrm{I}}/(\sqrt{2\pi}x^{1-\lambda})$ used by Sinclair et al. [26]).

To summarize, the generalized stress intensity factor at a re-entrant corner of a specimen loaded in mode I condition can be computed by means of the H-integral (27). The values of the complementary stresses and displacements are provided by Eqs. (28) and (29), whereas the values of the actual stresses and displacements have to be computed by a FEA. The integration path Γ is arbitrary; therefore it can be chosen at a certain distance from the stress singularity, i.e. the notch tip, where the solution provided by standard FEAs breaks down.

5. Comparison with performed experiments

Aiming to prove the soundness of the present approach, comparisons with *ad hoc* experiments as well as with data available in the literature are provided. Concerning ad hoc experiments, a series of tests with notched three-point flexure specimens made of polystyrene was carried out.

The specimen geometry is as in Fig. 2. The thickness t was equal to 3.7 mm (which is enough to achieve plane strain conditions); the length l and the height b were, respectively, 76 mm and 18 mm. The notch depth d was 1.8 mm, i.e. the relative notch depth was 1/10. Specimens were machined with three notch angles ω: 60°, 120° and 150°. For each geometry five specimens were prepared and tested. Five plane specimens were also tested to obtain the tensile strength value σ_u, which was found to be equal to 70.6 MPa. Finally, note that the notch root radius was kept very small for each specimen (the maximum value was 0.02 mm for the geometry with $\omega = 60°$): since this is more than one order of magnitude less than the finite crack extension (19) it is assumed that the notch radius did not affect the experimental results, and, therefore, the notch can be considered sharp as in the theoretical analysis of Sections 3 and 4.

In order to apply criteria of the kind of Eq. (8), the generalized SIF is needed. Therefore, FEAs were carried out by the LUSAS® code for each geometry, followed by the computation of the H-integrals as outlined in the previous Section. Exploiting symmetry, only half of the specimens were analyzed. Details of the mesh used as well of the integration path chosen for the specimen with $\omega = 120°$ can be seen in Fig. 9. Note that, wishing to have a more complete description of the effect of the notch opening angle, the generalized SIFs were computed also for geometries that were not tested, i.e. for ω equal to 0°, 30°, 90°.

By means of dimensional analysis, it is possible to write the generalized SIF as

$$K_{\mathrm{I}}^{*} = \frac{Pl}{tb^{1+\lambda}} f\left(\frac{l}{b}, \frac{d}{b}, \omega\right) \tag{30}$$

where f is the so-called shape function. Since the slenderness and the relative notch depth were kept constant for all the specimens, in the following the shape function will be considered just a function of the notch opening angle, i.e. $f = f(\omega)$. Therefore, by means of the generalized SIFs (Eq. (27)) and of the relationship (30), the values of the shape function $f(\omega)$ have been computed every 30° in the interval 0–180°.

Eq. (30) in critical conditions becomes:

$$K_{\mathrm{Ic}}^{*} = \frac{P_{\mathrm{cr}}^{\omega} l}{tb^{1+\lambda}} f(\omega) \tag{31}$$

and, if $\omega = 180°$, yields:

$$\sigma_u = \frac{P_{\mathrm{cr}}^{\pi} l}{tb^{2}} f(\pi) \tag{32}$$

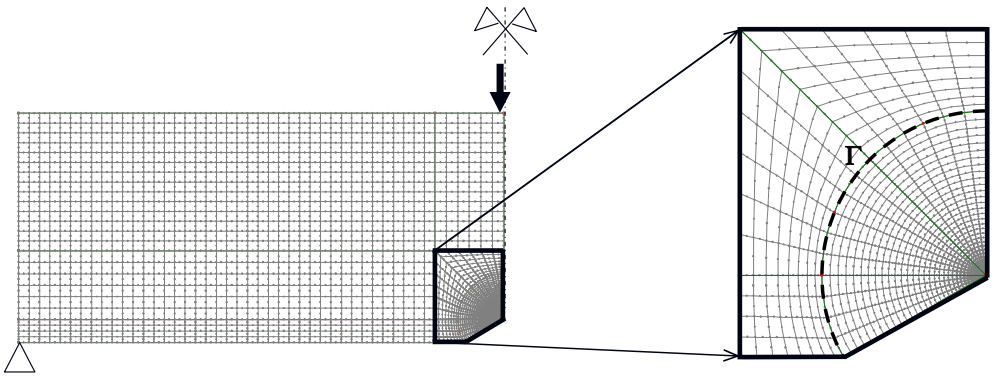

Fig. 9. Computation of the generalized SIF for the specimen with a notch opening angle equal to $\omega = 120°$. Mesh for the FEA and detail of the integration path Γ (dashed line).

where the value $f(\pi)$ (equal to 1.782 for the given geometry) can be found in structural mechanics classical books (it provides the maximum normal stress in an un-notched TPB specimen). P_{cr}^{ω} and P_{cr}^{π} are respectively the failure load for a notch opening angle equal to ω and equal to 180°. Taking the ratio side by side of Eqs. (31) and (32) and using the expression (20) of the generalized fracture toughness provided by the coupled FFM criterion derived in Section 3, yields:

$$\frac{P_{cr}^{\omega}}{P_{cr}^{\pi}} = \xi(\omega)\frac{f(\pi)}{f(\omega)}s^{2(1-\lambda)} \tag{33}$$

where the brittleness number defined in Eq. (10) appears. The ratio between the failure loads for a notched and an un-notched specimen is therefore function only of the opening angle and of the brittleness number. In Fig. 10 the relative failure loads are plotted versus ω for various values of s. The curves with low brittleness numbers refer to a more brittle structural behavior: they are more sensitive to the stress singularity at notch tip and hence show a faster decay of the failure load on decreasing the notch opening angle.

Eq. (33) as well as Fig. 10 clearly show that brittleness does not depend uniquely on the material, as already observed in Section 3. In fact, by the definition of s (Eq. (10)), a relatively ductile material can provide a brittle structural response for sufficiently large structural size and vice-versa. For a review about the significance of the brittleness number in structural mechanics, see [5].

Interestingly, all the curves in Fig. 10 show a minimum for notch opening angles larger than zero, an effect which is frequently met in experiments. Note that the minimum becomes more pronounced for higher values of s.

Finally, observe that curves with brittleness numbers too high (or, in terms of FFM, structures where the ratio between the finite crack extension and the ligament length is not much smaller than unity) have not been drawn in Fig. 10 since, in such cases, the assumptions made in the derivation of the present FFM criterion (e.g. considering only the asymptotic stress field) are no longer acceptable.

In order to check the predictive capability of the FFM criteria, beyond the tensile strength, also the fracture toughness is required. This was not obtained experimentally. Thus, for the present case, a best fit procedure exploiting the data of all the notched specimens was used to get the value of the toughness (note that an analogous procedure was used in [24]): $K_{Ic} = 2.23\text{MPa}\sqrt{\text{m}}$ and, consequently, $s = 0.236$. Results are presented in

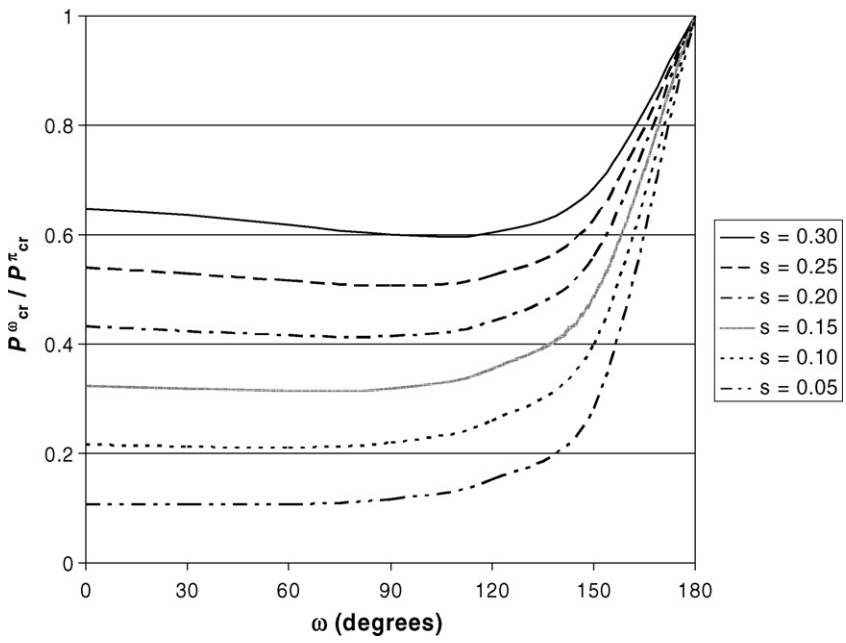

Fig. 10. Relative failure loads of the TPB polystyrene specimens vs. notch opening angle for different values of the brittleness number s.

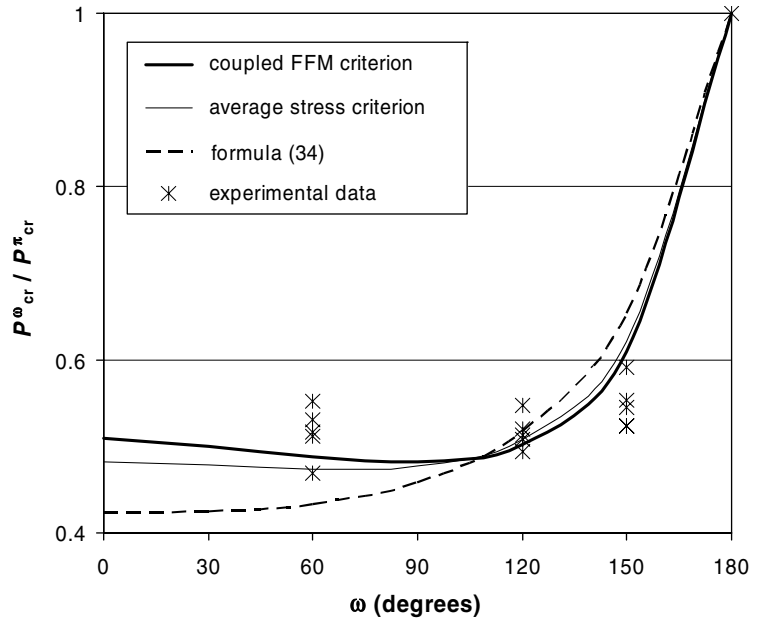

Fig. 11. Relative failure loads of the TPB polystyrene specimens vs. notch opening angle: experimental data (crosses) and predictions according to the coupled FFM criterion (thick line), the average stress criterion (thin line) and formula (34) (dashed line).

Fig. 11, together with the predictions provided by the average stress criterion (Eqs. (8) and (9)) and by the fitting formula proposed in [6]:

$$\frac{P^{\omega}_{\mathrm{cr}}}{P^{\pi}_{\mathrm{cr}}} = \left(\frac{P^{0}_{\mathrm{cr}}}{P^{\pi}_{\mathrm{cr}}}\right)^{2(1-\lambda)} \tag{34}$$

where P^{0}_{cr} is the failure load of the cracked specimen. Obviously, a best fit is needed for each failure criterion, yielding three different values of the fracture toughness. Fig. 11 shows that the FFM coupled criterion provides the best results. Formula (34), which is a monotonic function of the notch opening angle, is very easy to apply since it does not require the knowledge of the generalized SIF; however, in the present case, it provides the worst predictions.

6. Comparison with experimental data from the literature

The FFM criterion has been applied also to the data obtained in [3,24]. Concerning the former data, they were obtained testing PMMA specimens under flexure load having a geometry similar to that of our specimens (see Fig. 2). The dimensions were as follows: thickness $t = 50$ mm; length $l = 290$ mm; height $b = 50$ mm; notch depth $d = 20$ mm, i.e. the relative notch depth was 4/10. Specimens were prepared with a notch opening angle ω, respectively equal to: 0°, 45°, 90°, 120°, 150° and 180°. For each geometry three specimens were tested.

Also in this case, a FEA was performed by using the LUSAS® code for each geometry. Then, by means of the H-integral, the generalized SIFs were evaluated leading to the values of the shape function f to be inserted into Eq. (33).

Observe that, since Carpinteri [3] tested plain as well as cracked specimens, both tensile strength and fracture toughness were determined experimentally and there was no need to perform a best fit procedure as in the previous case. A brittleness number equal to 0.0693 was found: note that the structural response is much more brittle than the one obtained in Section 5, since specimen size was larger and PMMA has a higher strength and a lower toughness with respect to polystyrene (i.e. PMMA is more brittle than polystyrene).

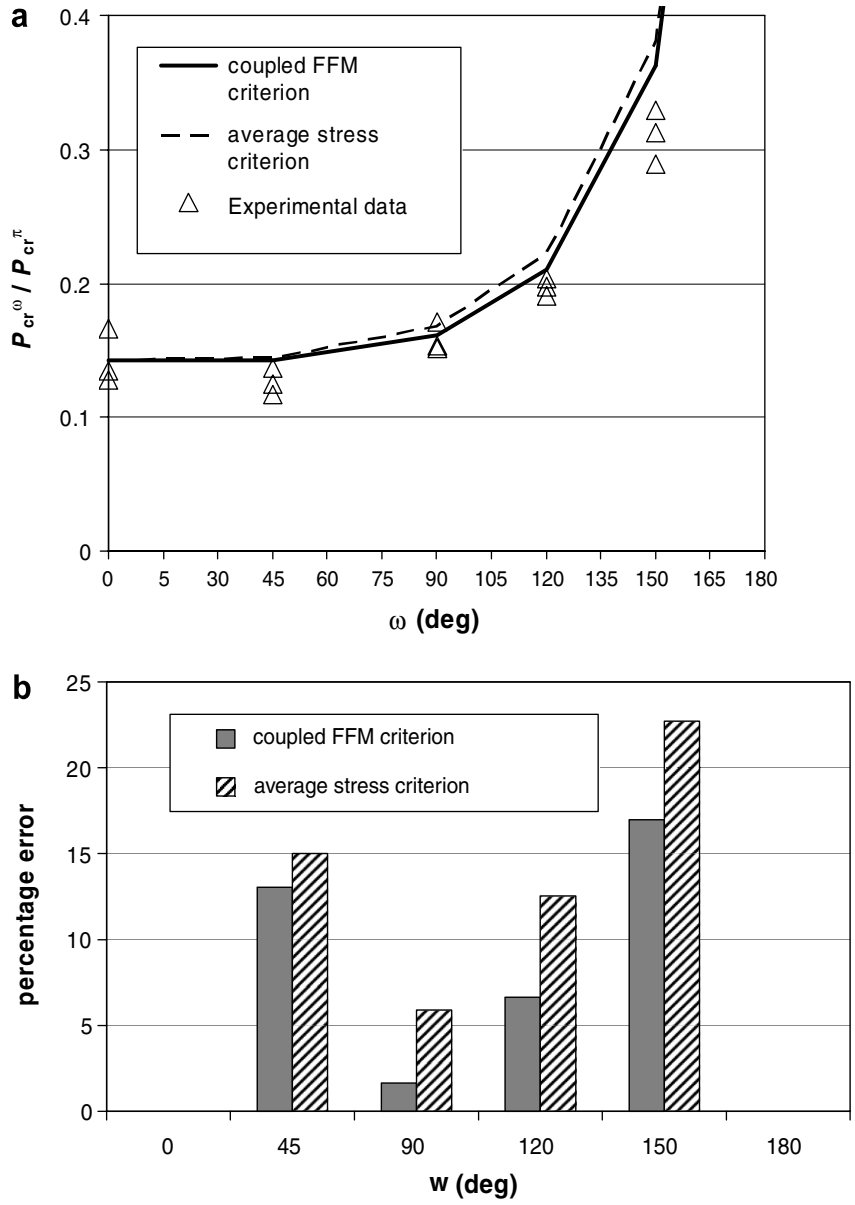

Fig. 12. (a) Relative failure loads of PMMA specimens tested in Carpinteri [3] vs. notch opening angle: experimental data (triangles) and predictions according to the FFM coupled criterion (continuous line) and the average stress criterion (dashed line). (b) Percentage errors of the two criteria with respect to the average values of the experimental data.

The relative failure load is then provide by Eq. (33). Results are presented in Fig. 12, together with predictions provided by the average stress criterion. Observe that, in this case, formula (34) provides results very close to the average stress criterion and therefore it has not been drawn within Fig. 12.

Fig. 12b shows that the coupled FFM criterion provides the best results for all the geometries. Note that both the criteria tend to overestimate the failure loads; the maximum percentage error is about 17% for the coupled FFM criterion while it rises to 23% for the average stress criterion.

Carpinteri [3] tested also PMMA specimens with a relative notch depth equal to 2/10: in this case, we found that the coupled FFM predictions are better than the average stress estimates for three of the four values of re-entrant corners tested.

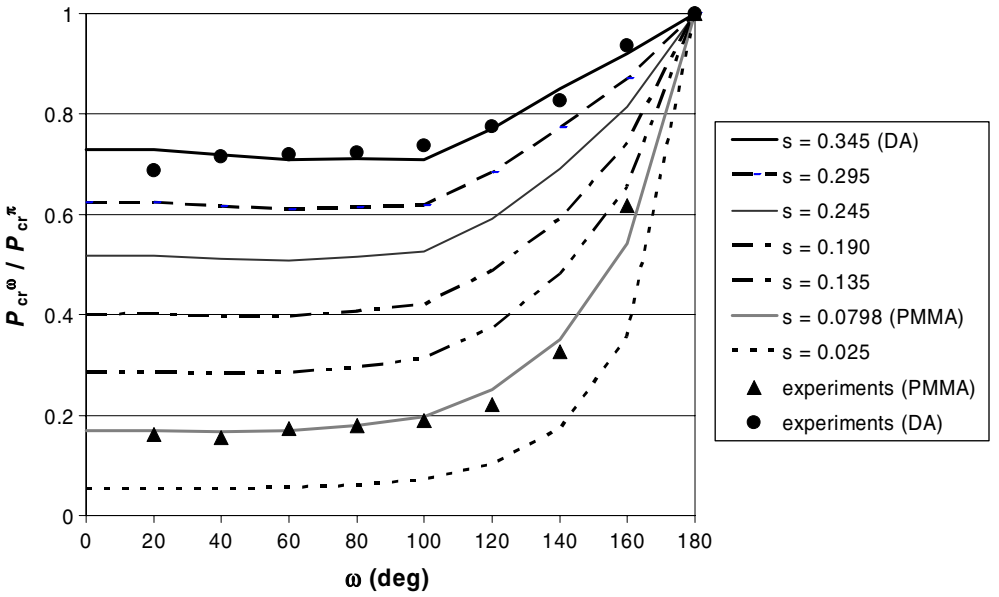

Fig. 13. Relative failure loads of PMMA and DA specimens tested in Seweryn [24] vs. notch opening angle: experimental data (triangles for PMMA and circles for DA) and predictions according to the FFM coupled criterion for different values of the brittleness number s.

Finally, the coupled FFM criterion has been applied to the data obtained by Seweryn [24] from double edge notched specimens with nine different notch opening angles (from 20° to 180° every 20°) under tensile load. Interestingly, for each geometry, he tested three specimens made of PMMA and two made of duraluminum (DA). In the same paper, the experimental data were compared with the predictions obtained by the average stress criterion, after the toughness of the two materials and the generalized SIFs had been determined, respectively by a best fit procedure and by FEAs.

In Fig. 13, the theoretical predictions obtained by the FFM coupled criterion are plotted for several s values, according to Eq. (33). The different curves relate to specimens with the same geometry but different material property: predictions for PMMA specimens refer to a brittleness value $s = 0.0798$ whereas predictions for the DA specimens refer to $s = 0.345$. In the same figure also the experimental data are represented by means of the average relative failure loads, for the sake of clarity. It is interesting to point out there is a rather good agreement between theory and experiments both for a very brittle material, i.e. PMMA, and for a less brittle one, DA. However, it should be noted that, for these data, also the average stress criterion provides satisfactory results (see [24]).

7. Conclusions

- A fracture criterion involving both stress requirements and energy balances is implemented to predict the failure of specimens containing sharp V-shaped notches.
- The criterion is capable of predicting experimental data on the effect of notch opening angle, in three different materials: two brittle polymers and duraluminum.
- Predictions obtained using this criterion are better than the ones given by the classical average stress criterion.

References

[1] Blom A, Hedlund A, Zhao W, Fathulla A, Weiss B, Stickler R. Short fatigue crack growth behaviour in Al2024 and Al7475. In: Miller K, de los Rios E, editors. The behaviour of short fatigue cracks. London: MEP; 1986. p. 36–66.
[2] Carpinteri A. Static and energy fracture parameters for rocks and concretes. Mater Struct 1981;14:151–62.

[3] Carpinteri A. Stress-singularity and generalized fracture toughness at the vertex of re-entrant corners. Engng Fract Mech 1987;26:143–55.
[4] Carpinteri A. Cusp catastrophe interpretation of fracture instability. J Mech Phys Solids 1989;37:567–82.
[5] Carpinteri A, Cornetti P, Barpi F, Valente S. Cohesive crack model description of ductile to brittle size-scale transition: dimensional analysis vs. renormalization group theory. Engng Fract Mech 2003;70:1809–39.
[6] Carpinteri A, Pugno N. Fracture instability and limit strength conditions in structures with re-entrant corners. Engng Fract Mech 2005;72:1254–67.
[7] Cornetti P, Pugno N, Carpinteri A, Taylor D. Finite fracture mechanics: a coupled stress and energy failure criterion. Engng Fract Mech 2006;73:2021–33.
[8] Dunn M, Suwito W, Cunningham S. Fracture initiation at sharp notches: correlation using critical stress intensities. Int J Solid Struct 1997;34:3873–83.
[9] Gómez F, Elices M. Fracture of components with V-shaped notches. Engng Fract Mech 2003;70:1913–27.
[10] Hashin Z. Finite thermoelastic fracture criterion with application to laminate cracking analysis. J Mech Phys Solids 1996;44:1129–45.
[11] Hazenberg J, Taylor D, Lee T. Mechanisms of short crack growth at constant stress in bone. J Biomech 2006;27:2114–22.
[12] Hillerborg A, Modéer M, Petersson P. Analysis of crack formation and crack growth in concrete by means of fracture mechanics and finite elements. Cement Concrete Res 1976;6:773–82.
[13] Karihaloo B, Abdalla H, Xiao Q. Size effect in concrete beams. Engng Fract Mech 2003;70:979–93.
[14] Kashtanov A, Petrov Y. Fractal models in fracture mechanics. Int J Fract 2004;128:271–6.
[15] Kim S, Nairn J. Fracture mechanics analysis of coating/substrate systems. Part I: Analysis of tensile and bending experiments. Engng Fract Mech 2000;65:573–93.
[16] Kinloch A, Shaw S, Tod D, Hunston D. Deformation and fracture behaviour of a rubber-toughened epoxy: 1. Microstructure and fracture studies. Polymer 1983;24:1341–54.
[17] Lazzarin P, Zambardi R. A finite-volume-energy based approach to predict the static and fatigue behavior of components with sharp v-shaped notches. Int J Fracture 2001;112:275–98.
[18] Leguillon D. Strength or toughness? A criterion for crack onset at a notch. Eur J Mech A/Solids 2002;21:61–72.
[19] Leguillon D, Yosibash Z. Crack onset at a V-notch. Influence of the notch tip radius. Int J Fracture 2003;122:1–21.
[20] Morozov N. Mathematical problems of a crack theory (in Russian). Moscow: Nauka; 1984.
[21] Neuber H. Theory of notch stresses. Berlin: Springer; 1958.
[22] Novozhilov V. On a necessary and sufficient condition for brittle strength. Prik Mat Mek 1969;33:212–22.
[23] Pugno N, Ruoff N. Quantized fracture mechanics. Philos Mag A 2004;84:2829–45.
[24] Seweryn A. Brittle fracture criterion for structures with sharp notches. Engng Fract Mech 1994;47:673–81.
[25] Seweryn A. A non-local stress and strain energy release rate mixed mode fracture initiation and propagation criteria. Engng Fract Mech 1998;59:737–60.
[26] Sinclair G, Okajima M, Griffin J. Path independent integrals for computing stress intensity factors at sharp notches in elastic plates. Int J Numer Meth Engng 1984;20:999–1008.
[27] Tada H, Paris P, Irwin G. The stress analysis of cracks. Handbook. second ed. St Louis, MO, USA: Paris Productions Incorporated; 1985.
[28] Taylor D. Geometrical effects in fatigue: a unifying theoretical model. Int J Fatigue 1999;21:413–20.
[29] Taylor D, Cornetti P, Pugno N. The fracture mechanics of finite crack extension. Engng Fract Mech 2005;72:1021–38.
[30] Taylor D, Merlo M, Pegley R, Cavatorta M. The effect of stress concentrations on the fracture strength of polymethylmethacrylate. Mater Sci Engng A 2004;382:288–94.
[31] Tovo R, Livieri P, Benvenuti E. An implicit gradient type of static failure criterion for mixed-mode loading. Int J Fract 2006;141:497–511.
[32] Whitney J, Nuismer R. Stress fracture criteria for laminated composites containing stress concentrations. J Compos Mater 1974; 8:253–65.